

Impact of effective capture cross section on generation-recombination rate in InAs/GaAs quantum dot solar cell

Ahna Sharan¹, Jitendra Kumar

Department of Electronics Engineering, Indian Institute of Technology (Indian School of Mines) Dhanbad
Jharkhand-826004, E-mail: ¹ahna.129@gmail.com

Abstract- Quantum dot solar cell structures have been theoretically analysed to study the impact of effective capture cross sections on quantum dot generation-recombination processes. The Poisson's and continuity equation were solved self-consistently to obtain electrostatic potential, electron and hole carrier distribution, and electron filling of the QDs. The occupation probability of the QDs was used to estimate the effective capture cross-sections under different doping and bias condition.

I. INTRODUCTION

The concept of using an intermediate energy level holds great promise in extending the efficiency of single-junction solar cell beyond the Shockley-Quiesser limit [1]. The use of an intermediate band (IB) helps in harnessing below-gap photons to generate additional photocurrent. The discrete energy levels of InAs/GaAs quantum dots (QDs) have been utilised as an IB to develop quantum dot solar cell (QDSC). Despite being widely researched, a significant potential for improvement still exists in QDSC. One of the main limitations of QDSC is the recapture of excited electrons from the conduction band (CB) to the IB, which aggravates recombination in the device and reduces open-circuit voltage (V_{oc}) [2]. The higher value of electron and hole capture cross-sections (CSs) are the underlying cause of such V_{oc} degradation.

In this work, we have analysed the variation of effective capture CS along the intrinsic region and its effect on CB to valence band (VB) generation and recombination through the QD intermediate energy level. The device characteristics of the QDSC were obtained by self consistently solving the Poisson's and continuity equation. We observed that doped QDs tend to modify the effective capture CS significantly. First, we examined the effect of doping on effective capture CS and then analysed its impact on IB generation rate under various bias condition.

II. THEORETICAL FORMULATION

The band structure and device characteristics of the QDSC was obtained by solving the 1-D drift-diffusion model, which includes the following sets of equation [3]:

$$\frac{d^2 \varphi}{dx^2} = \frac{-q(p-n-fN_I+N_{ID}+N_D-N_A)}{\epsilon_s} \quad (1)$$

where φ is the electrostatic potential, q is the electronic charge, ϵ_s is the permittivity of the medium, n and p are electron and hole carrier concentration, respectively, f is the occupation probability of the IB, N_{ID} is the dopant density of

the IB, N_D is the density of donor impurities, and N_A is the density of acceptor impurities.

$$\frac{dJ_n}{dx} = q(G_{CV} + G_I - R_{CV} - R_{SRH}) \quad (2a)$$

$$\frac{dJ_p}{dx} = q(G_{CV} + G_I - R_{CV} - R_{SRH}) \quad (2b)$$

where $J_{n(p)}$ is the electron (hole) current density, G_{CV} is the carrier generation rate from VB to CB, G_I is the generation-recombination (G-R) rate through the IB, R_{CV} is the recombination between the CB and the VB and R_{SRH} is the Shockley Read Hall recombination.

The net IB generation rate, G_I is expressed as [3], [4]:

$$G_I = \frac{N_I v_{th} \left[\sigma_e g_{VI} n_i e^{-\frac{E_I^0 - E_i^0}{kT}} + \sigma_h g_{CI} n_i e^{-\frac{E_i^0 - E_I^0}{kT}} + g_{CI} g_{VI} - \sigma_e \sigma_h (pn - n_i^2) \right]}{\sigma_e g_{VI} n_i e^{-\frac{E_I^0 - E_i^0}{kT}} + \sigma_h g_{CI} n_i e^{-\frac{E_i^0 - E_I^0}{kT}} + g_{CI} + g_{VI} + \sigma_e n + \sigma_h p} \quad (3)$$

The detail about all the terms used in (3) is given in Table I.

TABLE I
PARAMETERS USED IN SIMULATION

Parameters	Value
IB energy, E_I^0	1.122 eV
Intrinsic energy, E_i^0	0.749 eV
Intrinsic carrier concentration, n_i	$2.3 \times 10^6 \text{ cm}^{-3}$
Thermal velocity, v_{th}	10^7 cm/s
IB Density of states, N_I	$8 \times 10^{16} \text{ cm}^{-3}$
Light generation coefficient: VB to IB, g_{VI}	$2.31 \times 10^{-4} \text{ cm}^{-1}$
IB to CB, g_{CI}	$2.31 \times 10^{-4} \text{ cm}^{-1}$
Hole capture CS, σ_h	$1.25 \times 10^{-15} \text{ cm}^2$
Electron capture CS, σ_e	$1.25 \times 10^{-12} \text{ cm}^2$
Emitter dopant density, N_A	$5 \times 10^{18} \text{ cm}^{-3}$
Base dopant density, N_D	$3 \times 10^{17} \text{ cm}^{-3}$
IB dopant density, N_{ID}	$32 \times 10^{16} \text{ cm}^{-3}$

The Poisson's and continuity equation defined in (1) and (2), respectively, are solved iteratively using the Newton Raphson method. The solution at equilibrium was taken as an initial guess. The equations were numerically discretised through Scharfetter-Gummel (SG) scheme [5]. The estimates of electron and hole capture CS given in Table I are obtained from the electron capture lifetime from CB to IB when the IB level is completely empty and IB to VB when the IB level is completely full, respectively [3]. The effective capture cross sections are modulated by the change in the occupation probability, f , of the QDs under illumination and applied bias.

III. RESULTS AND DISCUSSION

In this work, we study two QDSC structure: QDSC-A is undoped, whereas, in QDSC-B, the interdot space is considered to be n-type δ -doped with dopant density, N_{ID} $32 \times 10^{16} \text{ cm}^{-3}$. Fig. 1 shows the band structure of the undoped and doped device at short circuit condition without

illumination, where InAs/GaAs QD layers are stacked in the i-GaAs region. The energy band diagram for the QDSC-A exhibits a high and constant electric field. In contrast, QDSC-B is characterised by a high electric field near the p-side and flat band along the rest of the depletion region. Another significant observation for QDSC-B is that the intermediate energy level falls below the Fermi level for many of the QDs, leading to prefilled states in the QD. The prefilled QDs help in repelling the recapture of electrons from the CB.

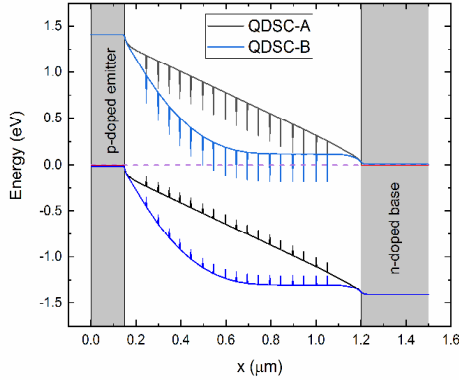


Fig. 1. Band diagram of the QDSC-A and QDSC-B at short circuit condition without illumination

Recombination through the QD dominates over SRH and CB to VB radiative recombination at higher bias voltage. Hence, the analysis of G_T , which accounts for both generation and recombination through the QD intermediate energy level, is an essential aspect in determining the device performance. Fig. 2 shows the effective capture CSs and generation rate for undoped and doped QDs under short circuit illuminated conditions. The effective capture CSs are relatively constant in QDSC-A except near the n-doped base, where electrons are injected into the QDs from the base region. In QDSC-B, the electron distribution along the intrinsic region is changed due to doping. The potential barrier formed around the QDs due to prefilled levels prohibits electron recapture into the QDs,

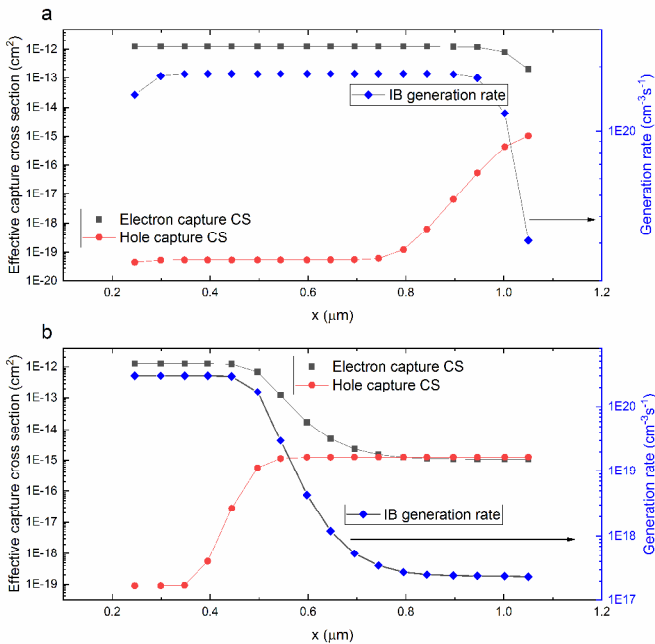


Fig. 2: Effective electron and hole capture cross sections and generation rate for a) QDSC-A and b) QDSC-B at illuminated short circuit conditions

leading to reduced electron capture CS. For both cases, the electron capture CS is low when the QD filling probability is high, and the reverse is true for hole capture CS. In QDSC-A, the IB generation rate is also constant except at the edge QDs following the curve of effective capture CS. In QDSC-B, the IB generation rate is high where the hole capture CS is low, even though the electron capture CS is high in that region. The reduced hole capture CS in this region helps in inhibiting the recombination of captured electrons into the VB. Towards the n-doped base, the generation rate decreases as the electron and hole capture CSs become comparable to each other, creating a clear passage for the captured electrons to recombine into the VB.

Fig. 3 shows the effective capture CSs and generation rate for doped QDSC under open circuit condition. The QDs now act as effective trap centers, and the recombination rate replaces the generation rate. The lower mobility of holes and reduced electric field at higher bias voltage restricts the escape of holes. Hence the hole capture CS is comparatively constant at open-circuit voltage, making the IB recombination rate entirely dependent on the electron capture CS.

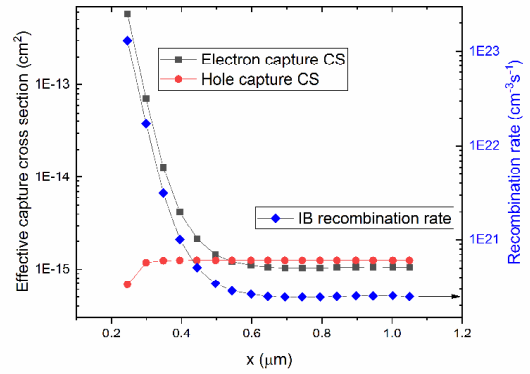


Fig. 3. Effective electron and hole capture cross sections and recombination rate for QDSC-B at open circuit condition

IV. CONCLUSION

We have presented an analysis of theoretically modelled QDSC structure, focusing on the impact of varying capture CSs on the QD G-R rate. The most desirable G-R rates are achieved when the electron and hole capture CSs are substantially different so that the captured electrons from the CB to the QDs are restricted from getting trapped into the VB.

REFERENCES

- [1] A. Luque and A. Martí, "Increasing the Efficiency of Ideal Solar Cells by Photon Induced Transitions at Intermediate Levels," *Phys. Rev. Lett.*, vol. 78, no. 26, pp. 5014–5017, June 1997.
- [2] F. Cappelluti, M. Giovannini, and A. Khalili, "Impact of doping on InAs/GaAs quantum-dot solar cells: A numerical study on photovoltaic and photoluminescence behavior," *Sol. Energy Mater. Sol. Cells*, vol. 157, pp. 209–220, May 2016.
- [3] Y. Gu, X. Yang, H. Ji, P. Xu, and T. Yang, "Theoretical study of the effects of InAs / GaAs quantum dot layer's position in i-region on current-voltage characteristic in intermediate band solar cells," vol. 101, no. 081118, August 2012.
- [4] A. Luque *et al.*, "Operation of the intermediate band solar cell under nonideal space charge region conditions and half filling of the intermediate band," *J. Appl. Phys.*, vol. 99, no. 094503, May 2006.
- [5] D. L. Scharfetter and H. K. Gummel, "Large-Signal Analysis of a Silicon Read Diode Oscillator," *IEEE Trans. Electron Devices*, vol. 16, no. 1, pp. 64–77, Jan 1969.